New isoreticular metal-organic framework materials for high hydrogen storage capacity

Tatsuhiko Sagara, Julia Ortony, and Eric Ganz[a)]
Department of Physics, University of Minnesota, Minneapolis, Minnesota 55455

(Received 25 July 2005; accepted 11 October 2005; published online 6 December 2005)

We propose new isoreticular metal-organic framework (IRMOF) materials to increase the hydrogen storage capacity at room temperature. Based on the potential-energy surface of hydrogen molecules on IRMOF linkers and the interaction energy between hydrogen molecules, we estimate the saturation value of hydrogen sorption capacity at room temperature. We discuss design criteria and propose new IRMOF materials that have high gravimetric and volumetric hydrogen storage densities. These new IRMOF materials may have gravimetric storage density up to 6.5 wt % and volumetric storage density up to 40 kg H_2/m^3 at room temperature. © *2005 American Institute of Physics*. [DOI: 10.1063/1.2133734]

I. INTRODUCTION

Hydrogen may be used as an energy carrier for fuel cell vehicles in the future. The development of onboard hydrogen storage in a safe, light, and cheap manner is underway. The US Department of Energy (DOE) has set targets of 4.5 wt % gravimetric hydrogen density and 36 kg H_2/m^3 volumetric hydrogen density for onboard use by 2007.[1] Recently developed metal-organic framework (MOF) materials are promising for their use in hydrogen storage if the storage properties are improved.[2–9] Yaghi and co-workers have developed the series of isoreticular (IR) MOF materials which consist of zinc oxide clusters connected by organic linker molecules.[2–5,10,11] These materials have nanoscale pores and large surface area, providing many hydrogen molecule binding sites. Several IRMOF materials have been tested for hydrogen storage at low temperatures (below 78 K), and the experiments and the theoretical calculations identified the hydrogen binding sites.[4,12–14] However, few results have been published for hydrogen storage by these materials at room temperature.[4,7] There is a need to design new materials for high hydrogen storage capacity at room temperature for fuel cell cars. In this study, we sample the potential-energy surface for H_2 on IRMOF-1 and investigate the interaction between hydrogen molecules. Based on these results, we estimate the saturation values of hydrogen sorption capacities at room temperature and reasonable pressure. We propose several new IRMOF materials that have high gravimetric and volumetric densities that meet the DOE targets for hydrogen storage at room temperature.

II. COMPUTATIONAL METHOD

Second order Møller-Plesset perturbation theory (MP2) calculations with the resolution of identity approximation (RI-MP2) were performed using the TURBOMOLE program.[15] Exact MP2 and coupled-cluster singles and doubles and noniterative triples [CCSD(T)] calculations were performed using the GAUSSIAN 03 program.[16] For multiple hydrogen binding-energy calculation, geometries were optimized using RI-MP2 method and the TZVPP basis set, and then single point energies were calculated using the QZVPP basis set. The CCSD(T) binding energies were estimated and corrected for the charge-transfer effect. As described previously,[17] we multiplied the RI-MP2/QZVPP binding energies by 0.77 to obtain the estimated CCSD(T) binding energy with the charge-transfer correction. For potential-energy-surface calculation, the MP2/TZVPP energies were multiplied by 0.76 to estimate the CCSD(T)/QZVPP energies with the charge-transfer correction. The calculations were carried out at the Minnesota Supercomputing Institute at the University of Minnesota.

III. RESULTS AND DISCUSSION

A. Potential-energy surface of H_2 molecule on the IRMOF-1 linker

In order to calculate the hydrogen sorption values of IRMOF materials over a wide range of temperatures and pressures, one must perform the grand canonical Monte Carlo (GCMC) simulations. The GCMC calculations with the traditional force fields are limited by the poor quality of potential-energy surface.[12] Therefore, there is a need for more accurate potential-energy surface calculations. In this study, we performed a potential-energy-surface scan for H_2 on IRMOF-1 linker using a lithium-terminated benzenedicarboxylate molecule ($BDCLi_2$) with MP2 and the TZVPP basis

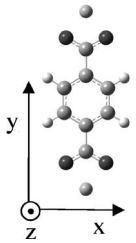

FIG. 1. Definition of x, y, and z axes of the $BDCLi_2$.

[a)]Electronic mail: ganzx001@umn.edu

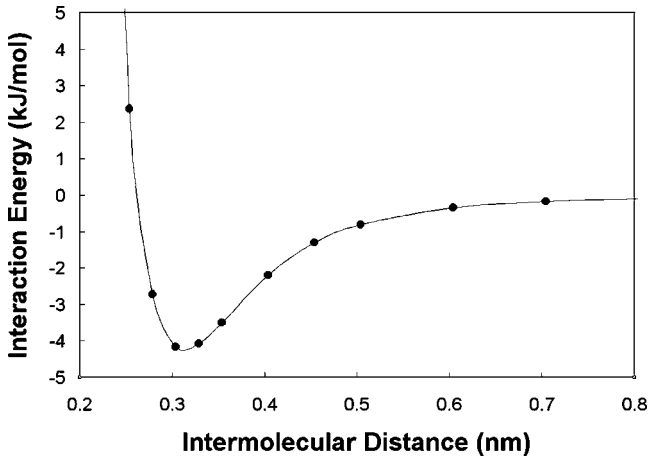

FIG. 2. Interaction energy between H_2 and $BDCLi_2$ as a function of z. The H_2 molecule is perpendicular to the $BDCLi_2$ molecular plane.

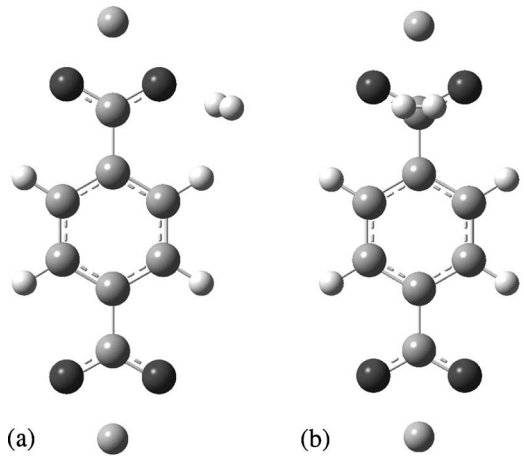

FIG. 4. Local minimum states of H_2 (a) near oxygen atom and (b) above carbon.

set. It is known that the MP2 method overestimates the binding energies in some van der Waals systems.[18–21] Previously, we calculated the correction factor for H_2 bound to an isolated benzene molecules and applied it for H_2 above the aromatic ring of IRMOF linkers.[17] For simplicity, we use the same correction factor for the entire linker, even though one might expect smaller correction factor above the oxygen atoms due to the contribution of electrostatic interactions.

We define the coordinate axis as shown in Fig. 1. The linker molecule is in the x-y plane, and the origin is at the center of the molecule. Figure 2 shows the interaction energy as a function of z where H_2 is on the center of the linker. The hydrogen molecule is perpendicular to the linker plane (aligned along z axis). There is a global minimum at $z=0.304$ nm. We call this binding site as the C_6 site. The binding energy is 4.16 kJ/mol.

We next performed the potential-energy-surface scan for H_2 over the linker. The distance from the linker to the H_2 was kept constant at $z=0.304$ nm. In Fig. 3, we show the potential-energy surface for three hydrogen orientations; H_2 aligned along the x, y, and z axes. For each orientation of the H_2, the minimum of the interaction energy is at the center of the aromatic ring. Compared to the other two orientations, there is a broad high-binding-energy site around the C_6 site for the H_2 aligned along the z axis. In our previous GCMC simulations on the IRMOF-1 at room temperature, the hydrogen binding on this area made significant contributions to the storage capacity.[12]

We also find two local minima for H_2, above oxygen atoms and above the carbon on the carboxylate group. Figure 4 shows the two optimized structures of H_2 on the linker. The binding energies are 3.36 and 2.77 kJ/mol, respectively. These are 81% and 67% of the binding energy of the C_6 site.

These potential-energy surfaces can be used in the grand canonical Monte Carlo simulations to calculate the sorption values at various temperature and pressure. The results could then be compared to the experimental results.

B. H_2–H_2 interaction

It is important to know how close the two hydrogen molecules can pack on the surface in order to estimate the number of H_2 molecules that large linkers can hold. In Fig. 5, we show the calculated interaction energy as a function of distance apart for two H_2 molecules in parallel configuration using RI-MP2 with the SVP, TZVPP, and QZVPP basis sets, and both MP2 and CCSD(T) with the aug-cc-pV5Z basis.

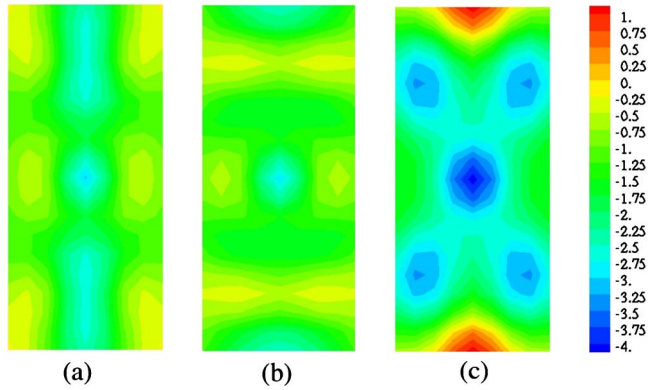

FIG. 3. Potential-energy surface (0.48×1.09 nm^2) of H_2 on $BDCLi_2$ at $z=0.304$ nm. H_2 is aligned along (a) x, (b) y, and (c) z axes.

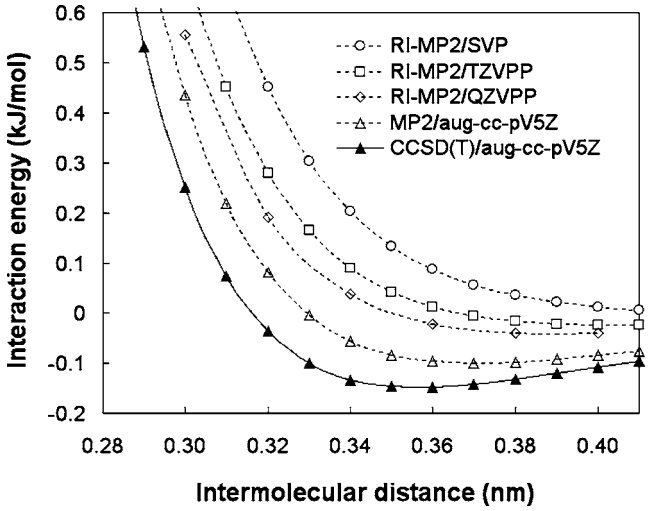

FIG. 5. H_2–H_2 interaction energy as a function of intermolecular distance. The two H_2 molecules are in parallel.

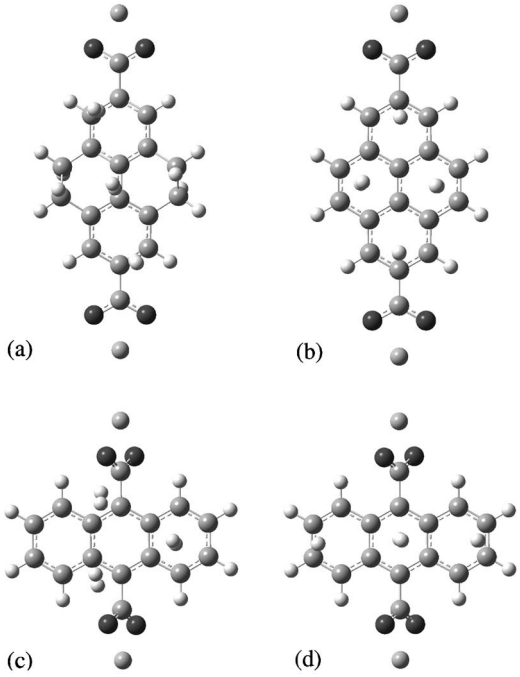

FIG. 6. Multiple hydrogen molecules on one side of the IRMOF linkers. (a) Three H_2 on the IRMOF-12 linker, (b) four H_2 on the IRMOF-14 linker, and (c) and (d) three H_2 on the IRMOF-993 linker.

Diep and Johnson pointed out that the MP2 results with smaller basis sets tend to overestimate the repulsive force compared to the more accurate CCSD(T) method.[22,23] The geometry optimization with the RIMP2/TZVPP method will overestimate the hydrogen intermolecular distance on the IRMOF linkers. These results will be used in Sec. III D to estimate the saturation coverage in the IRMOF materials.

C. Multiple H_2 binding on the IRMOF linkers

We calculated the multiple hydrogen binding energies on one side of the linker molecules although we note the H_2 can be bound on both sides of the linkers. In Fig. 6 we show the optimized structures for H_2 on IRMOF-12, IRMOF-14, and IRMOF-993. We show the total binding energy and average binding energy per H_2 in Table I. The IRMOF-12 linker can bind two to three hydrogen molecules, the IRMOF-993 linkers can bind three hydrogen molecules, and IRMOF-14 linker can bind four hydrogen molecules per side.

The IRMOF-12 linker can bind two H_2 molecules on the side aromatic rings and one on the above of the center carbon atoms. The first H_2 molecule is bound at a C_6 site with a binding energy of 5.50 kJ/mol. The second H_2 molecule goes to the other C_6 site with the same binding energy because these two H_2 molecules are located far apart. The third H_2 molecule is bound at the center of the molecule, with binding energy of 1.65 kJ/mol. This H_2 molecule pushes the other two H_2 molecules toward the outside of the linker. The average binding energy per H_2 is 4.22 kJ/mol.

The carboxylate groups in the IRMOF-993 linker are rotated 55° out of the anthracene plane. Because of this rotation, there are stable binding sites near the oxygen atoms in addition to the typical binding sites above the three aromatic rings. If three H_2 are located on one side of the linker molecule, two of them are located near the oxygen atoms, and the remaining H_2 is above the side aromatic ring, as shown in Fig. 6(c). This average H_2 binding energy is 4.71 kJ/mol, higher than 3.74 kJ/mol for three H_2 located above the aromatic rings as shown in Fig. 6(d).

The IRMOF-14 linker can bind four H_2 molecules per side. The first two H_2 molecules are bound on the C_6 sites of the aromatic rings attached to the caboxylate group with the binding energy of 4.87 kJ/mol. If four H_2 molecules are bound on one side of the IRMOF-14 linker, the H_2 molecules are located off center of the aromatic rings due to the repulsive interaction between H_2 molecules as shown in Fig. 6(b). The average distance between the adjacent hydrogen molecules is 0.32 nm (using RI-MP2/TZVPP). The average binding energy per H_2 is 4.12 kJ/mol. (The single hydrogen binding energy is 4.87 kJ/mol for H_2 above the end aromatic ring sites and 4.84 kJ/mol for H_2 above the central aromatic ring sites.)[17]

Thus, counting both sides, we find that these linker molecules can bind roughly two H_2 molecules per aromatic ring. At high pressure and room temperature, the saturation number of the bound H_2 molecules per side of small linkers will be same as the number of the aromatic rings in the linker molecules.

D. Designing new IRMOF materials for high hydrogen storage capacity at room temperature

We propose a method to estimate the saturation values of sorption capacities at room temperature and reasonable pres-

TABLE I. Calculated total binding energy in kJ/mol of multiple hydrogen molecules on one side of the linkers, average binding energy, and binding energies of first, second, third and fourth hydrogen molecules.

IRMOF	Total binding energy	Average binding energy	Binding energy for first H_2	Binding energy for second H_2	Binding energy for third H_2	Binding energy for fourth H_2
IRMOF-1	4.16	4.16	4.16			
IRMOF-3	4.72	4.72	4.72			
IRMOF-6	4.86	4.86	4.86			
IRMOF-8	8.23	4.12	4.54	3.69		
IRMOF-12	12.65	4.22	5.50	~5.50	~1.65	
IRMOF-14	16.47	4.12	4.87	~4.87	~3.42	~3.31
IRMOF-993	14.14	4.71	4.97	~4.97	~4.20	

TABLE II. Linker formula, one formula unit weight, estimated saturation number of bound H_2 molecules per linker, number of carbon atoms per bound H_2 molecules, estimated gravimetric storage capacity, mass density of the material, and estimated volumetric storage capacity of existing and new IRMOF materials at room temperature.

	Linker molecule formula	One formula unit weight (g/mol)	Estimated saturation number of bound H_2 molecules per linker	Number of carbon atoms per bound H_2 molecules	Estimated gravimetric storage capacity (wt %)	Mass density of the material (kg/m^3)	Estimated volumetric storage capacity ($kg\,H_2/m^3$)
IRMOF-1	$C_6H_4(CO_2)_2$	770	2	3.0	1.5	593	9
IRMOF-3	$C_6H_3NH_2(CO_2)_2$	815	2	3.5	1.5	628	9
IRMOF-6	$C_8H_6(CO_2)_2$	848	2	4.0	1.4	659	9
IRMOF-8	$C_{10}H_6(CO_2)_2$	920	4	2.5	2.6	448	12
IRMOF-12	$C_{16}H_{12}(CO_2)_2$	1154	4	2.6	2.1	381	8
IRMOF-14	$C_{16}H_8(CO_2)_2$	1142	8	2.0	4.1	373	16
IRMOF-993	$C_{14}H_8(CO_2)_2$	1070	6	2.3	3.3	825	28
IRMOF-M1	$C_6(NH_2)_4(CO_2)_2$	950	2	5.0	1.3	739	9
IRMOF-M2	$C_{18}H_{10}(CO_2)_2$	1221	8	2.3	3.8	581	23
IRMOF-M3	$C_{22}H_{10}(CO_2)_2$	1365	12	1.8	5.0	651	35
IRMOF-M4	$C_{28}H_{12}(CO_2)_2$	1587	12	2.3	4.4	756	35
IRMOF-M5	$C_{24}H_{10}(CO_2)_2$	1437	14	1.7	5.6	436	26
IRMOF-M6	$C_{32}H_{12}(CO_2)_2$	1731	20	1.6	6.5	554	39
IRMOF-M7	$C_{40}H_{14}(CO_2)_2$	2025	22	1.8	6.2	609	40

sure. This will help us to design new IRMOF materials that have high hydrogen sorption capacities in advance of synthesis or GCMC simulation.

We consider the potential-energy surface of H_2 on the IRMOF linkers and the interaction between H_2 molecules. In the previous section, we found that multiple hydrogen molecules can be located on a single side of the linker molecules. The average distance between the adjacent hydrogen molecules on the linkers is 0.32 nm at RIMP2/TZVPP level, where the H_2-H_2 interaction energy is 0.28 kJ/mol. Taking into account the overestimation of the repulsive interaction at this level of theory, we expect that the actual distance between hydrogen molecules on the linkers will be somewhat smaller than produced by the RI-MP2/TZVPP theory. At the CCSD(T)/aug-cc-p5Z level of theory, the intermolecular distance is 0.30 nm for the interaction energy of 0.28 kJ/mol. We, therefore, choose 0.30 nm as the closest distance between two H_2 on the IRMOF linkers.

We estimate the maximum number of H_2 molecules that can be bound to one side of the linkers at room temperature and reasonable pressure. We locate hydrogen molecules inside the edge of the aromatic ring and at least 0.30 nm away from each other. We count the number of hydrogen molecules on both sides of the linkers and estimated the volumetric and gravimetric sorption capacities of existing and new IRMOF materials (see Table II). We ignore the sorption at corner binding sites because our preliminary GCMC simulations on IRMOF-1 suggest that they are less important at room temperature.[12]

Although we have considered only one configuration, one can obtain the sorption capacities more accurately using GCMC or molecular-dynamics simulations that calculate the average of many possible configurations. Our purpose is to estimate the saturation values at room temperature and pressure around 50–100 atm in which saturation is desirable for application in fuel cell car. To this end, we only count strongly bound H_2 molecule configurations. At sufficient pressure, hydrogen molecules occupy all of the binding sites available on the linkers. For IRMOF-1, the BDC linker has one aromatic ring. If we assume that one linker molecule can hold two H_2 molecules (one H_2 on each side), then the estimated saturation value for IRMOF-1 crystal is 1.5 wt %. This is close to the experimental value of Pan *et al.* (1.65 wt %) at room temperature and 48 atm,[7] i.e., saturation appears to be roughly achieved under these conditions. We expect that saturation will be achieved for other materials around this pressure.

1. Increasing gravimetric density

For IRMOF-1, the BDC linker has one aromatic ring. If we assume that one linker molecule can hold two H_2 molecules (one H_2 on each side), then the estimated saturation value for IRMOF-1 crystal is 1.5 wt %. This is close to the experimental value of Pan *et al.* (1.65 wt %) at room temperature and 48 atm.[7] For IRMOF-3 and IRMOF-6, there are two binding sites per linker, and the saturation values are 1.5 and 1.4 wt %, respectively. The unsaturated experimental result for IRMOF-6 at room temperature and 10 atm is 1.0 wt %.[4]

As the number of the aromatic rings in the linkers increases, the number of binding sites increases. This can result in an improvement in the gravimetric sorption capacity. The IRMOF-8 linker can bind four H_2 molecules. The sorption capacity will be 2.6 wt %. The experimental result was 2.0 wt % at room temperature and 10 atm.[4] The IRMOF-12 linker can bind four H_2 molecules for a gravimetric density of 2.1 wt %. The IRMOF-993 linker can bind six molecules, leading to 3.3 wt %. Among the existing IRMOF materials, IRMOF-14 will have the best saturation value, 4.1 wt %.

We propose new IRMOF linkers as shown in Fig 7. We used the three-dimensional visualization capability of the CERIUS[2] program[24] to verify that the linkers fit in the space. Some examples of the three-dimensional structures are

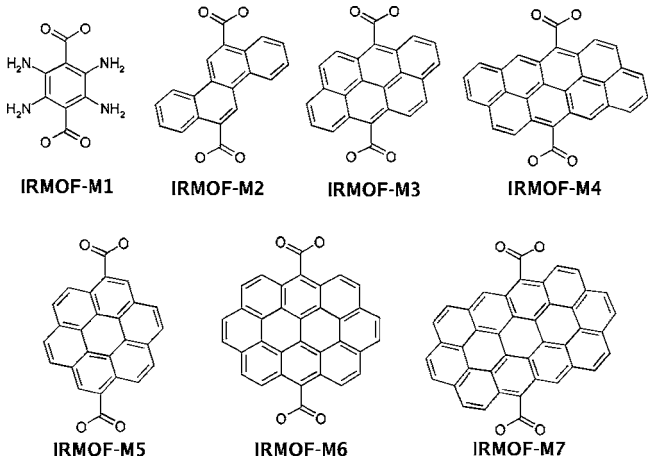

FIG. 7. Proposed linker molecules.

shown in Fig. 8. We used the CHIMERA program[25] to make these figures. Compared to IRMOF-M3, IRMOF-M4 has wider linker molecules. This increases the number of the binding sites but makes the pore size smaller and the diffusion of H_2 in the crystal slower.

IRMOF-M1 with tetra-amino benzenedicarboxylate linkers has the saturation values of 1.3 wt % gravimetric density and 9 kg H_2/m^3 volumetric density. This has very high binding energy, 5.55 kJ/mol.[17] IRMOF-M2 has chrysenedicarboxylate linker molecules which have four aromatic rings and can bind eight hydrogen molecules. We estimate the possible gravimetric and volumetric densities to be 3.8 wt % and 23 kg H_2/m^3, respectively. IRMOF-M3 and -M4 have the linkers of anthanthrenedicarboxylate and dibenzoanthanthrenedicarboxylate. We can locate 12 hydrogen molecules on these linkers (Fig. S1, sample packing).[26] The saturation values are 5.0 and 4.4 wt %, respectively. IRMOF-M5, -M6, and -M7 have coronenedicarboxylate, ovalenedicarboxylate, and tribenzoovalenedicarboxylate linkers, respectively. These linkers can bind 14, 20, and 22 H_2 molecules, leading to the saturation values of 5.6, 6.5, and 6.2 wt %, respectively.

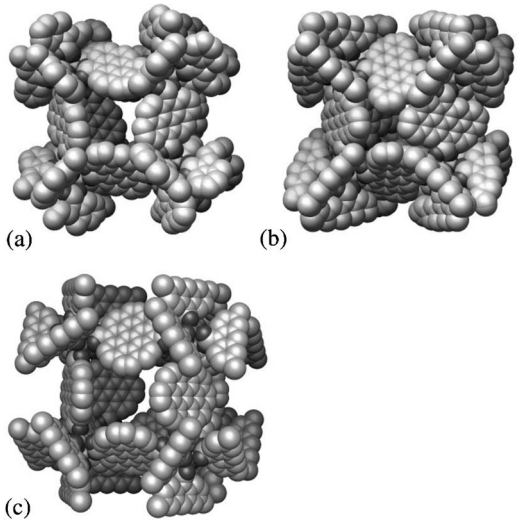

FIG. 8. Three-dimensional models of IRMOF-M3, IRMOF-M4, and IRMOF-M6.

To optimize the gravimetric storage density, one wants to minimize the mass required for each bound H_2 molecules. We count the number of carbon atoms needed to bind one hydrogen molecule. For IRMOF-3 and IRMOF-M1, we also count nitrogen atoms as carbon. For IRMOF-1, there are two bound H_2 molecules and six carbon atoms on the linker except for carboxylate groups. Then, the number of the carbon atoms per bound H_2 molecules is 3.0. The numbers for the IRMOF materials discussed here are shown in Table II. As one increase the size of the linker, each carbon atom tends to be shared for multiple binding sites. As a result, larger linkers have fewer carbon atoms per binding site, and therefore improved the gravimetric storage capacity. As the size of the linker increases, the relative contribution of H_2 binding on zinc oxide corners becomes less important.

2. Increasing volumetric density

There are two ways to increase the saturation volumetric density of hydrogen in IRMOF materials: (1) use wide linkers so the linkers can fill in the empty pore space or (2) use interpenetrating (catenated) structures. The IRMOF-993 linker has two extra aromatic rings on the sides of the IRMOF-1 linkers. This three-ring wide linker can hold three hydrogen molecules per side. This increases the volumetric density by a factor of 3 compared to IRMOF-1. We estimate the saturation capacity to be 28 kg H_2/m^3. Compared to IMOF-8, the linkers of IRMOF-M2, IRMOF-M3, and IRMOF-M4 have extra two, four, and six aromatic rings, respectively, within the same volume. In saturation, IRMOF-M2, IRMOF-M3, IRMOF-M4 can bind roughly 8, 12, and 12 hydrogen molecules, respectively. These lead to the estimated saturation volumetric sorption capacities of 23, 35, and 35 kg H_2/m^3, respectively.

Longer and wider linkers can be used. The linkers of IRMOF-M5, -M6, and -M7 are coronenedicarboxylate, ovalenedicarboxylate, and tribenzo-ovalenedicarboxylate, respectively. We estimate the saturation numbers of the hydrogen per side of these linker to be 14, 20, and 22, leading to saturation volumetric densities of 26, 39, and 40 kg H_2/m^3, respectively.

Interpenetrating structures such as IRMOF-11 and IRMOF-13 (Ref. 4) will also have higher volumetric density. The saturation volumetric densities are 16 and 32 kg H_2/m^3, respectively.

E. Graphene

We can estimate the saturation coverage for an isolated graphene sheet covered on both sides with the H_2 molecules with the spacing of 0.3 nm. At room temperature and sufficient pressure, the estimated saturation coverage will be 64% since the spacing between aromatic rings is 0.24 nm. This leads to a remarkable 9.2 wt % gravimetric storage density.

We can also estimate the volumetric density for a stack of graphene sheets. We choose a 0.9 nm separation between sheets so that hydrogen layers are 0.3 nm apart. The estimated saturation value of volumetric densities is 92 kg H_2/m^3. This provides an upper limit for the volumetric storage capacity of graphene-based materials.

We can also consider the sandwich structure with one H_2 layer between graphene sheets 0.6 nm apart. This leads to doubling binding energy; gravimetric and volumetric storage densities are reduced to 4.9 wt % and 70 kg H_2/m^3.

IV. SUMMARY

We have sampled the potential-energy surface for H_2 on the IRMOF-1 linker. This result can be used to calculate the sorption values at various temperatures and pressures using the grand canonical Monte Carlo simulations. The interaction between hydrogen molecules is studied. In saturation at room temperature, the distance between H_2 is 0.30 nm on the IRMOF linkers. Based on this distance and the potential-energy surface, we estimate the saturation values for the gravimetric and volumetric hydrogen densities at room temperature and high pressure. We propose new IRMOF material with high hydrogen storage capacity at room temperature. The estimated saturation gravimetric and volumetric densities of IRMOF materials can be up to 6.5 wt % and 40 kg H_2/m^3, respectively. This suggests that these materials should be useful for hydrogen storage in fuel cell cars. We look forward to seeing the experimental tests of these materials.

ACKNOWLEDGMENTS

This research has been supported by the University of Minnesota Supercomputing Institute for Digital Simulation and Advanced Computation and by a University of Minnesota Initiative on Renewable Energy and the Environment Hydrogen Cluster seed Grant No. SG-H2-2005.

[1] DOE website at http://www.eere.energy.gov/hydrogenandfuelcells/storage/
[2] J. L. C. Rowsell and O. M. Yaghi, Microporous Mesoporous Mater. **73**, 3 (2004).
[3] M. Eddaoudi, J. Kim, N. Rosi, D. Vodak, J. Wachter, M. O'Keeffe, and O. M. Yaghi, Science **295**, 469 (2002).
[4] N. L. Rosi, J. Eckert, M. Eddaoudi, D. T. Vodak, J. Kim, M. O'Keeffe, and O. M. Yaghi, Science **300**, 1127 (2003).
[5] J. L. C. Rowsell, A. R. Millward, K. S. Park, and O. M. Yaghi, J. Am. Chem. Soc. **126**, 5666 (2004).
[6] X. Zhao, B. Xiao, A. J. Fletcher, K. M. Thomas, D. Bradshaw, and M. J. Rosseinsky, Science **306**, 1012 (2004).
[7] L. Pan, M. B. Sander, X. Huang, J. Li, M. Smith, E. Bittner, B. Bockrath, and J. K. Johnson, J. Am. Chem. Soc. **126**, 1308 (2004).
[8] G. Ferey, M. Latroche, C. Serre, F. Millange, T. Loiseau, and A. Percheron-Guégan, Chem. Commun. (Cambridge) **2003**, 2976.
[9] D. N. Dybtsev, H. Chun, and K. Kim, Angew. Chem., Int. Ed. **43**, 5033 (2004).
[10] N. L. Rosi, J. Kim, M. Eddaudi, B. Chen, M. O'Keeffe, and O. M. Yaghi, J. Am. Chem. Soc. **127**, 1504 (2005).
[11] T. Düren, L. Sarkisov, O. M. Yaghi, and R. Q. Snurr, Langmuir **20**, 2683 (2004).
[12] T. Sagara, J. Klassen, and E. Ganz, J. Chem. Phys. **121**, 12543 (2004).
[13] Q. Yang and C. Zhong, J. Phys. Chem. B **109**, 11862 (2005).
[14] F. M. Mulder, T. J. Dingemans, M. Wagemaker, and G. J. Kearley, Chem. Phys. **317**, 113 (2005).
[15] R. Ahlriches, M. Bär, H. P. Baron *et al.*, TURBOMOLE Version 5.7 (Karlsuhe, Germany, 2004); R. Ahlrichs, M. Bär, M. Häser, H. Horn, and C. Kölmel, Chem. Phys. Lett. **162**, 165 (1989).
[16] M. J. Frisch, G. W. Trucks, H. B. Schlegel *et al.*, GAUSSIAN 03, Revision C.1, Gaussian, Inc., Pittsburgh, PA, 2003.
[17] T. Sagara, J. Klassen, J. Ortony, and E. Ganz, J. Chem. Phys. **123**, 014701 (2005).
[18] M. O. Sinnokrot, E. F. Valeev, and C. D. Scherrill, J. Am. Chem. Soc. **124**, 10887 (2002).
[19] M. O. Sinnokrot and C. D. Scherrill, J. Phys. Chem. **108**, 10200 (2004).
[20] S. Tsuzuki, T. Uchimaru, K. Matsumura, M. Mikami, and K. Tanabe, Chem. Phys. Lett. **319**, 547 (2000).
[21] S. Tsuzuki, K. Honda, T. Uchimaru, M. Mikami, and K. Tanabe, J. Am. Chem. Soc. **124**, 104 (2002).
[22] P. Diep and K. Johnson, J. Chem. Phys. **112**, 4465 (2000).
[23] P. Diep and K. Johnson, J. Chem. Phys. **113**, 3480 (2000).
[24] Accelys, Inc., CERIUS^2 Version 4.8.1 (Accelys, Inc., San Diego, CA, 2003).
[25] C. Huang, G. S. Couch, E. F. Petterson, and T. E. Ferin, Pac. Symp. Biocomput **1**, 724 (1996).
[26] See EPAPS Document No. E-JCPSA6-123-709544 for one figure and four tables. This document can be reached via a direct link in the online article's HTML reference section or via the EPAPS homepage (http://www.aip.org/pubservs/epaps.html).